Stability Analysis Using Fractional-Order PI Controller in a Time-Delayed Single-Area Load Frequency Control System with Demand Response

Deniz KATİPOĞLU
Department of Electrical-Electronics Engineering, Aksaray University, 68100, Turkey
denizkatipoglu@aksaray.edu.tr

***Abstract*—The current study investigates the stability analysis based on gain and phase margin (GPM) using fractional-order proportional-integral (FOPI) controller in a time-delayed single-area load frequency control (LFC) system with demand response (DR). The DR control loop is introduced into the classical LFC system to improve the frequency deviation. Although the DR enhances the system's reliability, the excessive use of open communication networks in the control of the LFC results in time delays that make the system unstable. A frequency-domain approach is proposed to compute the time delay that destabilizes the system using GPM values and different parameter values of the FOPI controller. This method converts the equation into an ordinary polynomial with no exponential terms by eliminating the exponential terms from the system's characteristic equation. The maximum time-delay values at which the system is marginally stable are calculated analytically using the new polynomial. Finally, the verification of the time delays calculated is demonstrated by simulation studies in the Matlab/Simulink environment and the root finder (quasi-polynomial mapping-based root finder, QPmR) algorithm to define the roots of polynomials with exponential terms providing information about their locations.**

***Index Terms*—delay systems, frequency control, PI control, power system control, stability analysis.**

I. INTRODUCTION

The load frequency control (LFC) system aims to maintain a consistent frequency profile and control power flow between regions at pre-programmed values through balancing power generation and demand [1]. Due to the ecological crisis and depletion risk of the non-renewable energy sources, integration of renewable energy (RE) resources into power systems may have a detrimental impact on the system's dynamic behavior and operating performance and cause difficulties in frequency control [2-3]. Demand response (DR) is a critical instrument for next generation energy systems in reducing the negative impacts of renewable energy sources and regulating system frequency by resolving uncertainties in power generation and load demand fluctuations. That is owing to changing the consumption hours of demand-side controllable loads or controlling these loads through activating and deactivating them. Such a quick reaction capability enhances the dynamic performance of the LFC systems and the safety in the operation of the power system. As a result, fluctuations in load demand are reduced, and frequency deviations are fixed [4-7]. For the participation of the DR in the frequency regulation market, a considerable number of controllable loads are involved in frequency control through a company named Load Aggregator [8]. Thermostatically controlled loads such as HVAC, electric water heaters, refrigerators, freezers, and the fast-response vehicle-to-grid services may be given as examples of the controllable loads.

In an interconnected power system, measurement data and control commands should be transmitted mutually among the control center, power plants, and the DR, and the communication infrastructure is required to meet the performance needs of the system. Time delays in communication, adversely affecting the dynamics and stability of the LFC-DR system, may occur during the transmission of the command signal between the control system and the responding loads [9-10].

PI controllers are widely used to zeroize the steady-state errors and improve dynamic response in LFC-DR systems [11]. Fractional-order proportional-integral (FOPI) controllers with higher performance features such as superior disturbance rejection, high-frequency noise immunity, and the elimination of the steady-state errors have become a popular control technology [12-13]. However, the FOPI controller has not been used in network-based communication and time-delayed LFC-DR systems [14-15]. In time-delayed LFC-DR systems, determining the maximum time-delay value at which the system will be marginally stable is also crucial in designing the controller and identifying the communication network type to achieve data transfer [16].

The maximum time delay of the LFC systems comprising a single-area electric vehicle collector (EV) in [17] and the microgrid frequency control system with a fixed communication delay in [18] was computed using the direct method proposed in the literature by Walton and Marshall [19]. In addition, the impacts of time delay in load frequency control for double-area LFC systems with DR in [20] and microgrid-based smart-power-grid-systems in [21] were calculated using the Rekasius substitution method [22]. The maximum time delay of LFC systems was also identified successfully using Lyapunov's stability theory and linear matrix inequalities methodology [23]. Besides H_∞ sliding mode controller was proposed in a time delayed load frequency control systems [24]. The approaches were used in the research indicated above when the LFC systems

Digital Object Identifier 10.4316/AECE.2023.02005

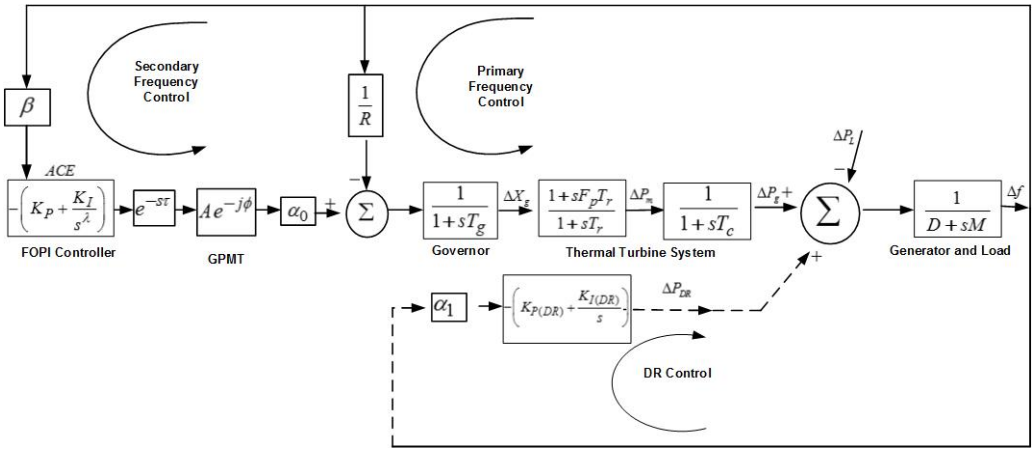

Figure 1. Block diagram of a time-delayed single-area LFC-DR system including a FOPI controller with added GPMT

comprised the traditional PI controllers. However, the maximum time delay computations can be more complex and burdensome in fractional-order systems. Thus, the fractional-order system [25] is converted into a classical polynomial of integer-order through a conversion equation to avoid such difficulties. The maximum time delay of the system can be determined using the exponential elimination approach [17] and Rekasius substitution method [22] once the system is converted to a classical polynomial. The first noteworthy contribution of this study is the application of an analytical approach [26] to compute the maximum time delay at which a single-area LFC-DR system with a FOPI controller will be marginally stable.

Although identifying the maximum time delay for stability is sufficient, any minor disturbance in the system may lead to instability, as steady and undamped oscillations in the frequency occur in practice after any disturbing influence in the time-delayed system. In addition to the margin stability, the time delay may also be calculated by adding other design parameters such as gain and phase margin (GPM) to achieve the desired performance. The gain and phase margin for various control applications were determined using the Nyquist stability criterion in the study [27]. Accordingly, the GPMT is added as a 'virtual compensator' to the forward transfer direction of the time-delayed LFC system model. The second significant contribution of this study is the calculation of the maximum time-delay values of a time-delayed single-area LFC-DR system with a FOPI controller for various fractional-order and controller parameter values using the exponential elimination method. The QPMR algorithm [28] and simulation tests in the time-domain [29] are used to verify the precision of the theoretical maximum time delays attained. Therefore, verifying the calculated GPMs-based maximum time-delay values with the QPMR algorithm is the third significant contribution of this study. The current study aims to investigate the impact of the FOPI controller fraction-order on the maximum time delay of the system and verify the theoretical results using simulation tests in the time-domain and the QPMR algorithm. When the fractional-order of the FOPI controller is smaller than one ($\lambda<1$), it is bigger than the results for $\lambda=1$; however, when the fractional-order of the FOPI controller is bigger than one ($\lambda>1$), then it is smaller. These results reveal that if the FOPI controller is used in a time-delayed LFC system, the fractional-order shall be preferred as less than one to build up the system stability. The second section of the study examines the model of the time-delayed single-area LFC-DR system comprising a FOPI controller with added GPMT. To calculate the time delay in the system, the details of the proposed method are given in the third section. The method is tested on a single-area LFC-DR control system in the fourth section, and the maximum time-delay values are computed for the diverse FOPI controller and fractional-order values. The results of the simulation studies in the time domain are provided accordingly. Finally, the fifth part confines conclusions and recommendations.

II. A Time-Delayed Single Area LFC-DR System with a FOPI Controller

Fig. 1 demonstrates the block diagram of a time-delayed single-area LFC-DR system comprising a FOPI controller with added GPMT. The system is modified by adding a time-delay and DR (dashed lines) to a standard single-area LFC system (continuous lines). In Fig. 1, A and ϕ refer to gain and phase margins. In addition, a proportional-integral type controller (PI) was used on the DR side [23]. The symbols in Fig. 1 such as Δ_f, ΔP_m ΔP_g, ΔP_{DR}, ΔP_L, and ΔX_g also denote the variations in system frequency, generator mechanical input power, generator output power, demand-side management power, system load, and valve position, respectively. For the system parameters, however M, D, T_g, T_c, T_r, F_P, β and R refer to the moment of inertia for a generator, damping coefficient of a generator, time constant for speed regulator, reheat-turbine time constant, reheat-turbine time coefficient, frequency orientation factor, and speed regulation coefficient, respectively. The participation factor coefficients indicated by a_0 and a_1 were used to identify the participation rate of the standard power generation unit and the DR control loop in the frequency modulation unit in the LFC system [30]. Also, K_P, K_I, and λ refer to the FOPI controller gain values and the fractional-order value of the integral controller. It should be noted that a fractional-order PI controller is obtained in the cases of $\lambda<1$ and $\lambda>1$, whereas a standard integer-order PI controller is acquired in the case of $\lambda=1$. In the standard LFC system with the DR added, time-delays may arise in the system during data transfer from the control center. Thus, a time delay is considered as much as the τ value during the measurements and data transmissions in the LFC-DR system, and it is denoted as $e^{-s\tau}$ in Fig. 1. The characteristic

equation of the time-delayed single-area LFC system comprising a FOPI controller with added GPMT is given below in (1).

$$\begin{aligned}&\Delta(s^{\lambda},\tau)=P(s)+Q(s)e^{-\tau s}Ae^{-j\phi}=0\\&=p_5s^{5+\lambda}+p_4s^{4+\lambda}+p_3s^{3+\lambda}+p_2s^{2+\lambda}+p_1s^{1+\lambda}\\&+p_0s^{\lambda}+(q_3s^{\lambda+2}+q_2s^{\lambda+1}+q_1s^2+q_0s)e^{-\tau s}Ae^{-j\phi}=0\\&=P'(s)+Q'(s)e^{-\tau s_{GPM}}=0\end{aligned}\tag{1}$$

In this formula,

$$\begin{aligned}&P(s,\lambda)=P'(s,\lambda)=p_5s^{5+\lambda}+p_4s^{4+\lambda}+p_3s^{3+\lambda}\\&+p_2s^{2+\lambda}+p_1s^{1+\lambda}+p_0s^{\lambda}p_5=MRT_gT_cT_r,\\&p_4=MRT_r(T_g+T_c)+MRT_gT_c+\mathrm{D}RT_gT_rT_c\\&+\alpha_1RK_{P(DR)}T_gT_rT_c,p_3=MR(T_g+T_c)+MRT_r\\&+DRT_r(T_g+T_c)+\mathrm{D}RT_gT_c+\alpha_1RK_{P(DR)}T_r(T_g+T_c)\\&+\alpha_1RK_{P(DR)}T_gT_c+\alpha_1RK_{I(DR)}T_gT_rT_c,p_2=MR\\&+DRT_r+DR(T_g+T_c)+\alpha_1RK_{P(DR)}(T_g+T_c)\\&+\alpha_1RK_{I(DR)}T_gT_c+\alpha_1RK_{I(DR)}T_r(T_g+T_c)+F_PT_r\\&+\alpha_1RK_{P(DR)}T_r,\ p_1=1+DR+\alpha_1RK_{P(DR)}+\alpha_1RK_{I(DR)}T_r\\&+\alpha_1RK_{I(DR)}(T_g+T_c),p_0=\alpha_1RK_{I(DR)}\\&Q'(s,\lambda)=Aq_3s^{\lambda+2}+Aq_2s^{\lambda+1}+Aq_1s^2+Aq_0s=q_3's^{\lambda+2}\\&+q_2's^{\lambda+1}+q_1's^2+q_0'sq_3'=A\alpha_0\beta RF_PT_rK_P,\\&q_2'=A\alpha_0\beta RK_P,q_1'=A\alpha_0\beta RF_PT_rK_I,\ q_0'=A\alpha_0\beta RK_{IS}\end{aligned}\tag{2}$$

It should be noted that the $e^{-s\tau}$ time-delay expression changes to $e^{-\tau s_{GPM}}$ in (1). Along with the $s=j\omega_c$, the system root of the imaginary-axis at the maximum time-delay value, the $e^{-\tau s_{GPM}}$ is given as $e^{-j\Phi}$ phase margin and the sum of the exponential term in (3).

$$\tau_{GPM}=\tau+\frac{\phi}{\omega_c}\tag{3}$$

There is no GPMT block diagram in the practical control systems. It is utilized as a virtual expression in the control system model to only analyze the system's dynamic performance at the desired GPM levels [27]. In (1), when the values are set to $A=1$ and, $\phi=0^o$ the original characteristic equation is calculated, in which the gain and phase margin has no effect in the system. When assessed (1) in terms of the GPM, three different states defined. These are: a) when $A=1$, only the effect of phase margin (ϕ) is observed, b) when, $\phi=0^o$ the characteristic equation can only be assessed by considering the gain margin, and c) the effect of both parameters on the system can be studies via changing both the gain and the phase margin in the system.

III. Calculation of GPM-Based Time Delay in a Time-Delayed Single-Area LFC-DR System with FOPI Controller

The method to calculate the time-delay values corresponding to the roots on the imaginary axis of the characteristic equation of a single-area LFC-DR system with added GPMT (Fig. 1) is described in detail in this section. In Fig. 1, if the roots crossing the imaginary-axis are denoted as $s=\pm j\omega_c$ in the GPMT-added system, the values of the time-delay corresponding to these roots are designated as τ_{GPM}. The τ also specify the time-delay values that produce the desired gain and phase margin. It is possible to analyze the stability of the system demonstrated in Fig. 1 by the position of the roots of the characteristic polynomial given in (1). For any value of time delay, all roots of a system must be on the left half-plane of the imaginary axis in order for it to be asymptotically stable. A time-delayed single-area LFC-DR system has infinite roots due to the exponential term in (1), and calculating such infinity is a difficult task. However, if the characteristic equation given in (1) has roots on the imaginary axis, these roots are much easier to compute, and thus it allows the maximum time delay of the system to calculate. Considering that there is a root imaginary axis on $s=j\omega_c$ equity for some finite values of $\Delta(j\omega_c+\tau_{GPM})=0$, then the $\Delta(-j\omega_c,\tau_{GPM})=0$ equation will have $s=-j\omega_c$ root for the same finite value due to the complex conjugative states of the roots. Thus, the calculation problem of the maximum time delay may be reduced to merely calculating the τ_{GPM} value using both $\Delta(j\omega_c,\tau_{GPM})=0$ and $\Delta(-j\omega_c,\tau_{GPM})=0$ equations [20-23]. For this purpose, the calculation of the time delay of the fractional-order characteristic equations with time-delay can be achieved as follows [26]. $\Delta(\sqrt[q]{s},\tau_{GPM})=0$ equation is used for a suitable conversion equation proposed by the characteristic equation of $\Delta(s^{\lambda},\tau_{GPM})=0$ given in (1) [28]; and if there is a solution for the $\Delta(s^{\lambda},\tau_{GPM})=0$ characteristic equation in the $s=j\omega_c$, then $\Delta(\sqrt[q]{-s},\tau_{GPM})=0$ equity can be used by (4) for $s=-j\omega_c$ complex conjugate root.

$$\begin{aligned}&\Delta(\sqrt[q]{s},\tau_{GPM})=P'(\sqrt[q]{s})+Q'(\sqrt[q]{s})e^{-s\tau_{GPM}}=0\\&\Delta(\sqrt[q]{-s},\tau_{GPM})=P'(\sqrt[q]{-s})+Q'(\sqrt[q]{-s})e^{s\tau_{GPM}}=0\end{aligned}\tag{4}$$

If $v=\sqrt[q]{s}$ variable is used as a simplified form in calculating the root crossing the imaginary-axis of the $\Delta(\sqrt[q]{s},\tau_{GPM})=0$ characteristic equation given in (4), a practical transformation is obtained to study the system stability.

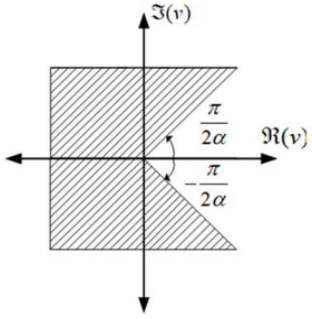

Figure 2. Stability domain in the plane of the fractional-order system

Based on this transformation, the stability domain defining the v plane shown in Fig. 2 and the new characteristic polynomial of the system are given in (5) and (6), respectively [24].

$$\left|\angle v\right|\le\frac{\pi}{2a},v\in\Re\tag{5}$$

$$\Delta(v,\tau_{GPM})=P'(v)+Q'(v)e^{-v^a\tau_{GPM}}=0\tag{6}$$

(7) is derived from (6) using the conjugate expression $\overline{v}$.

$$\Delta(\overline{v},\tau_{GPM})=P'(\overline{v})+Q'(\overline{v})e^{v^a\tau_{GPM}}=0\tag{7}$$

$\tau_{GPM}\in R^+$ or $s=\omega_ce^{\pm j\pi/2}$ is the complex roots of (4). As a result of the transformation process, the roots of (4) are derived as follows [24].

$$v=\sqrt[q]{s}=\sqrt[q]{\omega_c}e^{\pm j\pi/2a}\tag{8}$$

(9) without exponential terms is derived from (6) and (7)

to eliminate the exponential terms.

$$W(v) = P'(\overline{v})P'(v) + Q'(\overline{v})Q'(v) = 0 \quad (9)$$

If there is a solution of (4) in $s=j\omega_c$, it will also yield a solution for (9). (10) with ω is derived when $\overline{v} = (e^{-j\pi/a})v$ and $\overline{v} = \sqrt[a]{\omega_c}\, e^{j\pi/2a}$ equities are used in (9) [28].

$$W(\omega) = \left(P(e^{-j\pi/a}v)P'(v) + Q'(v)Q(e^{-j\pi/a}v)\right)\Big|_{v=\sqrt[a]{\omega_c}e^{j\pi/2a}} \quad (10)$$

Thus, the exponential term in (4) is removed by the exponential term elimination approach, as shown in (10). The positive real-root $\omega_c>0$ of (10) is equal to the root of (4) on the imaginary axis $s=\pm j\omega_c$. The following results may outcome based on the roots acquired from solving (10).

- The polynomial given by (10) may have no positive real-root for all $\tau_{GPM}\geq 0$ finite values. This means that there is no root on the imaginary axis of the single-area LFC-DR system with added GPMT given in (4), and the system proves that all roots in the characteristic equation in (4) are in the left half-plane of the imaginary axis. The time delay does not affect the system stability in this case, and the system is always stable and independent of time delay for all $\tau_{GPM}\geq 0$ finite values of time delay.
- (10) may have at least one positive real-root, indicating that the characteristic equation in (4) has at least a pair of $s=\pm j\omega_c$ complex conjugate roots on the imaginary axis. In this scenario, the stability of single-area LFC-DR system with added GPMT varies depending on the time delay, and the system is stable at τ_{GPM} value with the maximum time delay at the margin.

The maximum time-delay values at which the system will be stable are calculated using (11) via the positive real ω_c values attained from the solution of (10).

$$\tau_{GPM} = \frac{1}{v^{10}} tan^{-1}\left(\frac{I\left[(P'(v))/(Q'(v))\right]}{R\left[-(P'(v))/(Q'(v))\right]}\right)\Bigg| \quad (11)$$
$$v = \sqrt[a]{\omega_c}\, e^{j\pi/2a} + \frac{2k\pi}{\omega_c}; \quad k \hat{I} R^+$$

(10) specifies that the new characteristic polynomial must have a finite number of positive real-roots for all $\tau_{GPM} \in \Re^+$. (12) provides the set of these real-roots.

$$\{\omega_c\} = \{\omega_{c1}, \omega_{c2}, ..., \omega_{cq}\} \quad (12)$$

It is possible to calculate time-delay value ω_{cm}, $m=1,2,...,q$, τ_{GPM} for each positive real-root by (12). τ_{GPM} values generate a set of infinite time delays.

$$\{\tau_{GPMm}\} = \{\tau_{GPM1}, \tau_{GPM2}, ..., \tau_{GPMm,¥}\}, m = 1,2,...,q \quad (13)$$

In this equation, $\tau_{GPMm,r+1} - \tau_{GPMm,r} = 2\pi/\omega_c$ refer to iteration period. As a result, the maximum time-delay value of the control system with a GPMT is the minimum value in the time-delay set in (14) (τ_{GPMm}, $m=1,2,...,q$).

$$\tau_{GPM} = \min(\tau_{GPMm}) \quad (14)$$

After computing the maximum time-delay value of the time-delayed control system with a GPMT, (15) may be used practically to calculate the time-delay value that the original control system will have the desired gain and phase margin.

$$\tau = \tau_{GPM} - \frac{f}{\omega_c} \quad (15)$$

In this equation, while ϕ denotes the desired phase margin, ω_c refers to positive real-root crossing the imaginary-axis.

IV. Simulation and Results

The time-delay values of the LFC-DR system at the desired GPM values and varying gain and fraction-order values of the FOPI controller were determined in this section using the approach described in Chapter 3 while keeping the other system parameters constant. In addition, the accuracy of the proposed method and the outcomes were demonstrated using the QPMR algorithm, which is a numerical approach identifying the positions of the poles and zeros of the characteristic equation of any time-delayed system on the complex plane. The equations from Chapter 3 were used stepwise below to compute the time delay. The system parameters are as follows [31]:

$$M = 8.8,\ D = 1,\ F_P = 1/6,\ R = 1/11,\ \beta = 21,$$
$$T_g = 0.2, T_c = 0.3,\ T_r = 12,\ \mathrm{K}_{P(DR)} = 0.4,$$
$$\mathrm{K}_{I(DR)} = 0.6,\ \mathrm{K}_P = 0.4,\ \mathrm{K}_I = 0.6,\ \mathrm{A}=1,$$
$$\lambda=0.9,\ \phi=20^\circ, \alpha_0 = 0.6, \alpha_1 = 0.4.$$

Step 1: The characteristic equation of the time-delayed system comprising fractional-order degrees is derived through setting the system parameters in Fig. 1 into (1).

$$\begin{aligned}\Delta(s^\lambda, \tau_{GPM}) &= 0.576s^{5+0.9} + 4.9239s^{4+0.9} \\ &+10.6548s^{3+0.9} + 4.2504s^{2+0.9} + 1.3782s^{1+0.9} \\ &+0.0218s^{0.9} + (0.9164s^{2+0.9} + 0.4582s^{1+0.9} \\ &+1.3745s^2 + 0.6873s)e^{-s\tau_{GPM}} = 0\end{aligned} \quad (16)$$

As stated in (3), τ_{GPM} in this equation refers to the total expression of the system with time-delay value, taking into account the effect of phase margin in $\Phi=20^\circ=0.3491$ *rad* value and $s=j\omega_c$ equity; thus, the following formulation is conceivable.

$$\tau_{GPM} = \tau + \frac{0.3491}{\omega_c} \quad (17)$$

Step 2: As in (4), to express the characteristic equation attained in (16) in Step 1, $\Delta(\sqrt[a]{s}, \tau_{GPM}) = \Delta(\sqrt[10]{s}, \tau_{GPM}) = 0$ equity is structured as follows:

$$\begin{aligned}\Delta(\sqrt[10]{s}, \tau_{GPM}) &= 0.576(\sqrt[10]{s})^{59} + 4.923(\sqrt[10]{s})^{49} + 10.654(\sqrt[10]{s})^{39} \\ &+4.250(\sqrt[10]{s})^{29} + 1.378(\sqrt[10]{s})^{19} + 0.0218(\sqrt[10]{s})^{9} + (0.916(\sqrt[10]{s})^{29} \\ &+0.458(\sqrt[10]{s})^{19} + 1.374(\sqrt[10]{s})^{20} + 0.687(\sqrt[10]{s})^{10})e^{-s\tau_{GPM}} = 0\end{aligned} \quad (18)$$

It is also possible to formulate the same procedure as $\Delta(\sqrt[a]{-s}, \tau_{GPM}) = \Delta(\sqrt[10]{-s}, \tau_{GPM}) = 0$ for the complex conjugate root of the characteristic equation given in (18) above.

$$\begin{aligned}\Delta(\sqrt[10]{-s}, \tau_{GPM}) &= 0.576(\sqrt[10]{-s})^{59} + 4.9239(\sqrt[10]{-s})^{49} \\ &+10.654(\sqrt[10]{-s})^{39} + 4.250(\sqrt[10]{-s})^{29} + 1.378(\sqrt[10]{-s})^{19} \\ &+0.022(\sqrt[10]{-s})^{9} + (0.916(\sqrt[10]{-s})^{29} + 0.458(\sqrt[10]{-s})^{19} \\ &+1.374(\sqrt[10]{-s})^{20} + 0.687(\sqrt[10]{-s})^{10})e^{s\tau_{GPM}} = 0\end{aligned} \quad (19)$$

Step 3: To solve the new characteristic equation obtained in Step 2, the transformation equation $v = \sqrt[10]{s}$ was used as in (6). Furthermore, this transformation is also performed for the complex conjugate $\overline{v} = \sqrt[10]{-s}$.

$$\Delta(v,\tau_{GPM}) = 0.576(v)^{59} + 4.924(v)^{49} + 10.655(v)^{39} + 4.250(v)^{29} + 1.378(v)^{19} + 0.022(v)^{9} + (0.916(v)^{29} + 0.458(v)^{19} + 1.374(v)^{20} + 0.687(v)^{10})e^{-v^{10}\tau_{GPM}} = 0 \quad (20)$$

$$\Delta(\overline{v},\tau_{GPM}) = 0.576(\overline{v})^{59} + 4.924(\overline{v})^{49} + 10.655(\overline{v})^{39} + 4.250(\overline{v})^{29} + 1.378(\overline{v})^{19} + 0.022(\overline{v})^{9} + (0.916(\overline{v})^{29} + 0.458(\overline{v})^{19} + 1.374(\overline{v})^{20} + 0.687(\overline{v})^{10})e^{\overline{v}^{10}\tau_{GPM}} = 0 \quad (21)$$

Step 4: $\Delta(v,\tau_{GPM})=0$ and $\Delta(\overline{v},\tau_{GPM})=0$ equities attained by (20) and (21) in Step 3 eliminated the exponential term as given below.

$$\begin{aligned} W(v) &= P'(\overline{v})P'(v) + Q'(\overline{v})Q'(v) \\ &= (0.332e^{-j59\pi/10})v^{118} + (11.971e^{-j49\pi/10})v^{98} \\ &+ (73.254e^{-j39\pi/10})v^{78} + (\text{-}11.927e^{-j29\pi/10})v^{58} \\ &+ (\text{ -}0.394e^{-j49\pi/20})v^{49} + (\text{-}1.889e^{-j20\pi/10})v^{40} + \\ &(1.504e^{-j19\pi/10})v^{38} + (\text{-}0.098e^{-j29\pi/20})v^{29} \\ &+ (\text{-}0.472e^{-j\pi})v^{20} + (4.7603x10^{-4}e^{-j9\pi/10})v^{18} = 0 \end{aligned} \quad (22)$$

Step 5: By using (10), The equation below may be achieved if $v = \sqrt[10]{\omega_c}e^{j\pi/20} = \omega_c' e^{j\pi/20}$ (as $\omega_c' = \sqrt[10]{\omega_c}$) expression given in (22) in Step 4 is operated.

$$\begin{aligned} W(\omega'_c) &= 0.332\omega_c'^{118} + 11.971\omega_c'^{98} + 73.254\omega_c'^{78} \\ &\text{-}11.927\omega_c'^{58} \text{-}0.394\omega_c'^{49} \text{-}1.889\omega_c'^{40} + 1.504\omega_c'^{38} \\ &\text{-}0.099\omega_c'^{29} \text{-}0.472\omega_c'^{20} + 4.7603x10^{-4}\omega_c'^{18} = 0 \end{aligned} \quad (23)$$

Accordingly, 118 roots were calculated from the solution of the polynomial given by (23) above. Among 118 roots, however, only two positive real-roots as $\omega_c' = 0.9351 rad/s$ and $\omega_c' = 0.0317 rad/s$ were calculated. Since there was $\omega_c' = \sqrt[10]{\omega_c}$ relationship, the system's root crossing the imaginary-axis was calculated as $\omega_{c1}=0.5112$ *rad/s,* $\omega_{c2}=1.0247x10^{-15}$ *rad/s.*

Step 6: Using the attained $\omega_{c1}=0.5112$ *rad/s* and $\omega_{c2}=1.0247x10^{-15}$ *rad/s* positive real-roots in (11) and employing $v = \sqrt[10]{0.5112}e^{j\pi/20}$, $v = \sqrt[10]{1.0247x10^{-15}}e^{j\pi/20}$ conversions, the time-delay values in the system are calculated as $\tau_{GPM1}=1.0438s$, $\tau_{GPM2}=3.2192x10^{15}s$. Among these, the $\tau_{GPM}=\tau_{GPM1}=1.0438s$, which is the minimum time-delay value, is the maximum time-delay value of the system.

$$\tau_{GPM} = \frac{1}{v^{10}} tan^{-1}\left(\frac{\Im[(P'(v))/(Q'(v))]}{\Re[-(P'(v))/(Q'(v))]} \right) \Bigg| v = \sqrt[10]{\omega_c}e^{j\pi/20} \quad (24)$$

In this equity, $P'(v)$ and $Q'(v)$ polynomials are:

$$\begin{aligned} P'(v) &= 0.576(v)^{59} + 4.9239(v)^{49} + 10.6548(v)^{39} \\ &+ 4.2504(v)^{29} + 1.3782(v)^{19} + 0.0218(v)^{9}; \\ Q'(v) &= 0.9164(v)^{29} + 0.4582(v)^{19} \\ &+ 1.3745(v)^{20} + 0.6873(v)^{10} \end{aligned} \quad (25)$$

Step 7: The time-delay value calculated by (24) in Step 6 stands for the time-delay value of the LFC-DR system with a GPM. To find the time-delay value corresponding to the desired phase margin, the positive real-root $\omega_{c1}=0.5112$ *rad/s* calculated in Step 5 and the time-delay value in the desired gain-phase margin of the original LFC-DR system acquired by the time-delay value corresponding to this positive real-root in Step 6 can be formulated as follows while considering the phase margin as $\Phi=20^{\circ}=0.3491$ *rad.*

$$\tau = 1.0438 - \frac{0.3491 rad}{0.5112 rad/s} = 0.3609 s \quad (26)$$

For the desired GPM values and for a fractional-order controller in a time-delayed single-area LFC-DR system, stability analysis was performed in this study by following the processes outlined above.

This section analyses were done in three ways, as detailed below. Initially, the maximum time-delay values in the system were calculated for varying gain values and fractional-order values of the FOPI controller in the case of $A=1$, $\phi=0^{\circ}$. For this purpose, the aforementioned steps were executed at three different fractional values, $\lambda=0.9$, $\lambda=1$ and $\lambda=1.1$, by selecting the proportional controller gains as $K_p=0.1–0.5$ and the integral controller gains as $K_I=0.1–0.5$. Tables I, II, and III shows the calculated time-delay values for $\lambda=0.9$, $\lambda=1$ and $\lambda=1.1$, respectively. It was noteworthy that the classical integer-order PI ($\lambda=1$) controller was used in the system, according to Table II. When Table I for $\lambda=0.9$ compared to Table II for $\lambda=1$, the maximum time-delay values in all gain values of the PI controller were larger at $\lambda=0.9$ than at $\lambda=1$. This proved that the system stability was influenced positively at the $\lambda=0.9$ value, and the time-delay values that the system could tolerate after any disturbance effect are very high. However, when Table III for $\lambda=1.1$ and Table II for $\lambda=1$ were compared, lower time-delay values were found for all gain values of the PI controller in Table III among all PI controller gain-values. Therefore, it is conceivable to say that the system stability is negatively affected by the maximum time-delay values calculated for $\lambda=1.1$.

TABLE I. MAXIMUM TIME DELAYS FOR $\lambda = 0.9$ ($A=1$, $\phi=0^{\circ}$)

$\tau^*(s)$	K_I				
K_P	**0.1**	**0.2**	**0.3**	**0.4**	**0.5**
0.1	29.2429	9.7222	3.4331	1.7654	1.0857
0.2	29.4449	9.6720	3.4556	1.8940	1.2277
0.3	29.2047	9.2795	3.3728	1.9831	1.3353
0.4	28.4798	8.3789	3.2385	2.0326	1.4221
0.5	27.2195	6.6193	3.0657	2.0444	1.4838

TABLE II. MAXIMUM TIME DELAYS FOR $\lambda = 1$ ($A=1$, $\phi=0^{\circ}$)

$\tau^*(s)$	K_I				
K_P	**0.1**	**0.2**	**0.3**	**0.4**	**0.5**
0.1	19.2605	6.4331	2.3169	1.1373	0.6104
0.2	19.9402	6.6808	2.5272	1.3373	0.7859
0.3	20.3789	6.7078	2.6638	1.5065	0.9392
0.4	20.5229	6.4322	2.7238	1.6320	1.0722
0.5	20.3297	5.7621	2.7214	1.7280	1.1799

TABLE III. MAXIMUM TIME DELAYS FOR $\lambda = 1.1$ ($A=1$, $\phi=0^{\circ}$)

$\tau^*(s)$	K_I				
K_P	**0.1**	**0.2**	**0.3**	**0.4**	**0.5**
0.1	13.2415	4.2191	1.4608	0.5851	0.1683
0.2	14.0930	4.6511	1.7659	0.8223	0.3595
0.3	14.7898	4.9444	2.0154	1.0345	0.5398
0.4	15.3225	5.0733	2.2037	1.2180	0.7033
0.5	15.6475	4.9859	2.3327	1.3743	0.8542

Subsequently, the time-delay values for the desired GPM were calculated in the time-delayed LFC-DR system comprising a FOPI controller and with GPMT added in Fig. 1. The FOPI controller gain values in this scenario ranged between K_p=*0.1–0.5* and K_I=*0.1–0.5*. In addition, λ=*0.9* value was taken into account for the PI controller. First, the phase margin was kept constant at the $\phi=0^\circ$ value to assess the effect of the gain margin for the λ value indicated in the system, and the time-delay values of the gain margin *A=1*, *A=1.5* and *A=2* were given in Tables I, IV, and V. When compared to these tables, it was identified that the time-delay values decreased noticeably as the gain margin values *A=1*, *A=1.5* and *A=2* increased.

In the second scenario, the time-delay values for $\phi=0^\circ$, $\phi=10^\circ$, and $\phi=20^\circ$ were calculated while keeping the gain margin *A=1* constant to examine the effect of the phase margin on the time-delays for λ=*0.9*. The time-delay values for $\phi=0^\circ$, $\phi=10^\circ$, and $\phi=20^\circ$ at λ=*0.9* were presented in Tables I, VI, and VII. When these tables were analyzed, it was discovered that the time-delay values of all FOPI controller gain margin values decreased while the phase margin values increased. However, it was clear that the gain margin was more effective than the phase margin on the time-delay values, and the gain margin lowered the time-delay values more, according to the tables studied.

Finally, time-plane simulation studies were used to demonstrate the accuracy of the maximum time-delay values calculated when using a fractional-order controller in the LFC-DR system, and the dynamic performance of the LFC-DR system at the desired GPM values was investigated in the system.

TABLE IV. MAXIMUM TIME DELAYS FOR $\lambda = 0.9$ ($A = 1.5$, $\phi = 0^\circ$)

$\tau^*(s)$	K_I				
K_P	**0.1**	**0.2**	**0.3**	**0.4**	**0.5**
0.1	16.1050	3.4554	1.4403	0.7806	0.4432
0.2	15.9031	3.3728	1.6109	0.9537	0.5958
0.3	14.8309	3.1574	1.7097	1.0853	0.7265
0.4	11.8497	2.8900	1.7544	1.1818	0.8317
0.5	4.7308	2.6423	1.7549	1.2446	0.9137

TABLE V. MAXIMUM TIME DELAYS FOR $\lambda = 0.9$ ($A = 2$, $\phi = 0^\circ$)

$\tau^*(s)$	K_I				
K_P	**0.1**	**0.2**	**0.3**	**0.4**	**0.5**
0.1	9.6720	1.8940	0.8403	0.4164	0.1865
0.2	8.3789	2.0326	1.0438	0.5985	0.3470
0.3	4.9268	2.0373	1.1818	0.7448	0.4824
0.4	3.4979	1.9696	1.2573	0.8500	0.5913
0.5	2.8394	1.8704	1.2916	0.9241	0.6754

TABLE VI. MAXIMUM TIME DELAYS FOR $\lambda = 0.9$ ($A = 1$, $\phi = 10^\circ$)

$\tau^*(s)$	K_I				
K_P	**0.1**	**0.2**	**0.3**	**0.4**	**0.5**
0.1	26.6601	8.7015	2.8870	1.3293	0.6989
0.2	26.9419	8.7010	2.9311	1.4669	0.8459
0.3	26.8101	8.3815	2.8745	1.5666	0.9604
0.4	26.2237	7.5857	2.7671	1.6282	1.0549
0.5	25.1338	5.9774	2.6210	1.6534	1.1251

TABLE VII. MAXIMUM TIME DELAYS FOR $\lambda = 0.9$ ($A = 1$, $\phi = 20^\circ$)

$\tau^*(s)$	K_I				
K_P	**0.1**	**0.2**	**0.3**	**0.4**	**0.5**
0.1	24.0774	7.6807	2.3409	0.8933	0.3121
0.2	24.4389	7.7301	2.4065	1.0399	0.4641
0.3	24.4156	7.4834	2.3761	1.1501	0.5855
0.4	23.9677	6.7924	2.2956	1.2238	0.6876
0.5	23.0480	5.3356	2.1762	1.2623	0.7664

In Fig. 3, the LFC-DR system frequency response at the ΔP_d=*0.1pu* load variation was compared when there was no GPMT in the system (*A=1,* $\phi=0^\circ$) at the λ=*1.1* fractional-order of the controller, and the controller gains set as K_p=*0.3*, K_I=*0.3*. In addition, the configuration of the system roots at the specified time-delay values and the alteration in the system frequency response may be assessed using the QPMR algorithm in Fig. 3. The hypothetically calculated maximum time-delay value for λ=*1.1*, K_p=*0.3*, and K_I=*0.3* was τ=*2.0154s*. According to Fig. 3a, it was deduced from the configuration of the system roots that there was a complex root pairs in the left half-plane of the imaginary axis when lowered the time-delay value to τ=*1.8s<2.0154s*. Hence, the simulation studies verified the system stability, damping the oscillations in the system response. When Fig. 3b was examined, there was a complex root pair of the system at τ=*2.0154s* value on the imaginary axis. In this case, the system was stable at the margin, and undamped oscillations occurred in the frequency response. In Fig. 3c, however, the complex root pairs of the system were observed to be in the right half-plane of the imaginary axis, and there were undamped oscillations in the system response when increased the time-delay value to τ=*2.1s>2.0154s*.

The dynamic performance of the system was studied at the λ=*0.9* fractional-order of the FOPI controller by taking the GPM into consideration. The maximum time-delay value for K_p=*0.3*, K_I=*0.3* controller gain values of the single-area LFC-DR system at the fractional-order λ=*0.9* of the PI controller was computed as τ=*1.9831s* for *A=1*, $\phi=0^\circ$, as provided in Table I. This unit was the delay-value at which the oscillations in the system's frequency response were not damped and remained stable at the margin. However, such oscillations in frequency variation are intolerable in practical systems. The delay-value limit was set by adding the GPMT to the system to damped such amplitudes of oscillations in a short time and reach a steady state in the system. As demonstrated in Tables V and VII, the GPM-based time-delay values were calculated as τ=*0.7448s* and τ=*1.1501s* for *A=2*, $\phi=0^\circ$ and *A=1*, $\phi=20^\circ$ respectively. In addition, the simulation study of these delay values calculated in the GPMT parameters was given in Fig. 4. In contrast to the time-delay value derived by *A=1*, $\phi=20^\circ$ a state in Fig. 4, the oscillations in the frequency response were damped in a short time in the case of only phase margin (*A=1*, $\phi=20^\circ$). Similarly, the system oscillations were damped in a substantially shorter time when there was

only the gain margin ($A=1$, $\phi=0^{\circ}$). Furthermore, the oscillations in the selected gain margin were damped in a shorter period than the phase margin. These simulation studies proved that the gain and phase margin should be considered when computing the maximum time delay to improve the dynamic performance of the time-delayed LFC-DR systems.

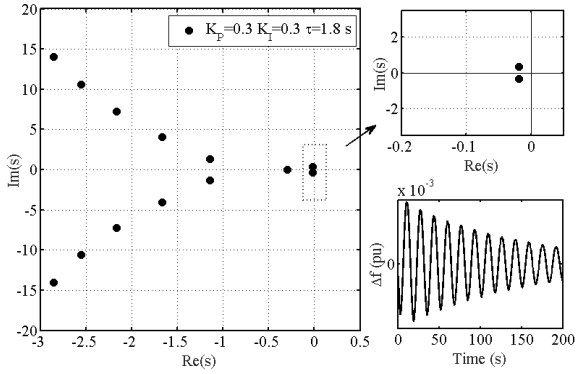

(a) $\tau = 1.8s$: Stable

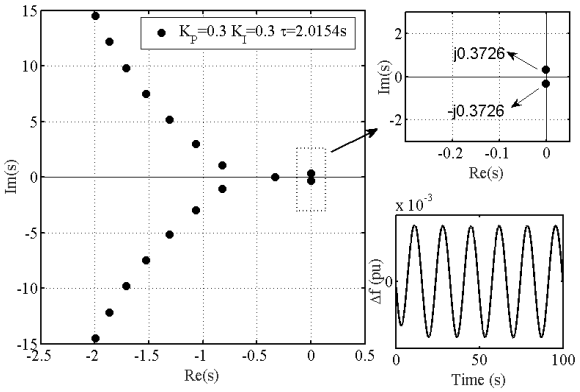

(b) $\tau = 2.0154s$: Marginally stable

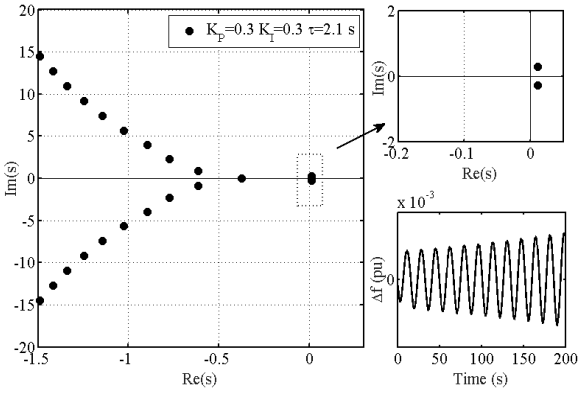

(c) $\tau = 2.1s$:Unstable

Figure 3. Location of the characteristic equation roots and frequency response of LFC-DR system for ($A=1$, $\phi=0^{\circ}$) $\lambda=1.1$

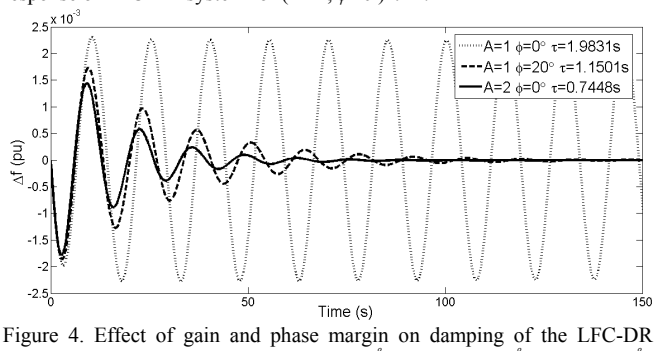

Figure 4. Effect of gain and phase margin on damping of the LFC-DR system frequency response for ($A=1$, $\phi=0^{\circ}$), ($A=1$, $\phi=20^{\circ}$), ($A=2$, $\phi=0^{\circ}$), $\lambda=0.9$, $K_p=0.3$, and $K_I=0.4$

V. CONCLUSIONS

This study used a single-area LFC-DR system with a communication delay FOPI controller to perform stability analysis by taking the GMP into account. An analytical method was used in the system to calculate the time delay for various fractional-orders of the controller and GPM parameters. Furthermore, simulation studies and the QPMR algorithm used widely in the literature demonstrated that the current method generated precise results. However, it may be more accurate to analyze the study findings under two different groups.

The maximum time delay results attained were greater than the results of the integer-order PI controller $\lambda=1$ when the fractional-order of the FOPI controller was less than one ($\lambda<1$); however, it was smaller when it was $\lambda>1$. These findings suggested that the fractional-order should be less than one to increase system stability when using a FOPI controller in a time-delayed LFC-DR system.

It may be sufficient to anticipate the maximum time delay information in the system. However, it is critical that the system operates beyond the stability margin and demonstrates the desired dynamic performance. The delay margin was calculated for the desired GPM parameters of the system by the proposed approach via adding the GMP parameters to the system. Therefore, the acquired results suggested that the system had a better dynamic performance at the desired GPM parameters.

In conclusion, this research results contributed to the literature by focusing on improving the system's dynamic performance and analyzing the effect of fractional-order controllers on the system's operating performance.

REFERENCES

[1] P. M. Anderson, A. A. Fouad, "Power System Control and Stability," pp. 3-11, John Wiley & Sons, 2008

[2] I. Muhammad, M. S. Shabbir, S. Saleem, K. Bilal, R. Ulucak, "Nexus between willingness to pay for renewable energy sources: Evidence from Turkey," Environmental Science and Pollution Research, vol. 28, no. 3, pp. 2972-2986, 2021. doi:10.1007/s11356-020-10414-x

[3] B. Vedik, R. Kumar, R. Deshmukh, S. Verma, C. K. Shiva, "Renewable energy-based load frequency stabilization of interconnected power systems using Quasi-Oppositional Dragonfly Algorithm," Journal of Control, Automation and Electrical Systems, vol. 32, no. 1, pp. 227-243, 2021. doi:10.1007/s40313-020-00643-3

[4] Z. A. Obaid, L. M. Cipcigan, L. Abrahim, M. T. Muhssin, "Frequency control of future power systems: reviewing and evaluating challenges and new control methods," Journal of Modern Power Systems and Clean Energy, vol. 7, no. 1, pp. 9-25, 2019. doi:10.1007/s40565-018-0441-1

[5] U. Ur Rehman, "A decentralized dynamic marketing-based demand response using electric vehicles in smart grid," Arabian Journal for Science and Engineering, vol. 45, pp. 6475-6488, 2020. doi:10.1007/s13369-020-04505-7

[6] Q. Shi, C. F. Chen, A. Mammoli, F. Li, "Estimating the profile of incentive-based demand response (IBDR) by integrating technical models and social-behavioral factors," IEEE Transactions on Smart Grid, vol. 11, no. 1, pp. 171-183, 2019. doi:10.1109/TSG.2019.2919601

[7] W. Huang, N. Zhang, C. Kang, M. Li, M. Huo, "From demand response to integrated demand response: Review and prospect of research and application," Protection and Control of Modern Power Systems, vol. 4, no. 1, pp. 1-13, 2019. doi:10.1186/s41601-019-0126-4

[8] F. Wang, X. Ge, K. Li, Z. Mi, "Day-ahead market optimal bidding strategy and quantitative compensation mechanism design for load aggregator engaging demand response," IEEE Transactions on Industry Applications, vol. 55, no. 6, pp. 5564-5573, 2019. doi:10.1109/TIA.2019.2936183

[9] S. A. Hosseini, M. Toulabi, A. S. Dobakhshari, A. Ashouri-Zadeh, A. M. Ranjbar, "Delay compensation of demand response and adaptive disturbance rejection applied to power system frequency control," IEEE Transactions on Power Systems, vol. 35, no. 3, pp. 2037-2046, 2019. doi:10.1109/TPWRS.2019.2957125

[10] V. P. Singh, P. Samuel, N. Kishor, "Impact of demand response for frequency regulation in two□area thermal power system," International Transactions on Electrical Energy Systems, vol. 27, no. 2, pp. 1-23, 2017. doi:10.1002/etep.2246

[11] H. Wang, J. Liu, F. Yang, Y. Zhang, "Proportional-integral controller for stabilization of second-order delay processes," International Journal of Control, Automation and Systems, vol. 12, no. 6, pp. 1197-1206, 2014. doi:10.1007/s12555-013-0341-0

[12] V. Çelik, M. T. Özdemir, K. Y. Lee, "Effects of fractional-order PI controller on delay margin in single-area delayed load frequency control systems," Journal of Modern Power Systems and Clean Energy, vol. 7, no. 2, pp. 380-389, 2019. doi:10.1007/s40565-018-0458-5

[13] S. Sondhi, Y. V. Hote, "Fractional order PID controller for load frequency control," Energy Conversion and Management, vol. 85, pp. 343-353, 2014. doi:10.1016/j.enconman.2014.05.091

[14] K. Bharti, V. P. Singh, S. P. Singh, "Impact of intelligent demand response for load frequency control in smart grid perspective," IETE Journal of Research, pp. 1-12, 2020. doi:10.1080/03772063.2019.1709570

[15] D. Katipoğlu, Ş. Sönmez, S. Ayasun, A. Naveed, "Impact of participation ratios on the stability delay margins computed by direct method for multiple-area load frequency control systems with demand response," Automatika, vol. 63, no. 1, pp. 185-197, 2022. doi:10.1080/00051144.2021.2020554

[16] S. Ayasun, "Computation of time delay margin for power system small-signal stability," European Transactions on Electrical Power, vol. 19, no. 7, pp. 949-968, 2009. doi:10.1002/etep.272

[17] A. Naveed, Ş. Sönmez, S. Ayasun, "Impact of electric vehicle aggregator with communication time delay on stability regions and stability delay margins in load frequency control system," Journal of Modern Power Systems and Clean Energy, vol. 9, no. 3, pp. 595-601, 2020. doi:10.35833/MPCE.2019.000244

[18] H. Gündüz, Ş. Sönmez, S. Ayasun, "Comprehensive gain and phase margins based stability analysis of micro-grid frequency control system with constant communication time delays," IET Generation, Transmission & Distribution, vol. 11, no. 3, pp. 719-729, 2017. doi:10.1049/iet-gtd.2016.0644

[19] K. Walton, J. E. Marshall, "Direct method for TDS stability analysis," IEE Proceedings D-Control Theory and Applications, vol. 134, no. 2, pp. 101-107, 1987

[20] D. Katipoğlu, Ş. Sönmez, S. Ayasun, A. Naveed, "The effect of demand response control on stability delay margins of load frequency control systems with communication time-delays," Turkish Journal of Electrical Engineering and Computer Sciences, vol. 29, no. 3, pp. 1383-1400, 2021. doi:10.3906/elk-2006-165

[21] C. A. Macana, E. Mojica-Nava, N. Quijano, "Time-delay effect on load frequency control for microgrids," 10th IEEE International Conference on Networking, Sensing and Control (ICNSC), pp. 544-549, 2013. doi:10.1109/ICNSC.2013.6548797

[22] Z. V. Rekasius, "A stability test for systems with delays," In Joint Automatic Control Conference, vol. 17, no. 39, 1980. doi:10.1109/JACC.1980.4232120

[23] N. Vafamand, M. H. Khooban, T. Dragičević, J. Boudjadar, M. H. Asemani, "Time-delayed stabilizing secondary load frequency control of shipboard microgrids," IEEE Systems Journal, vol. 13, no. 3, pp. 3233-3241, 2019. doi:10.1109/JSYST.2019.2892528

[24] S. K. Pradhan, D. K. Das, "H∞ performance-based sliding mode control approach for load frequency control of interconnected power system with time delay," Arabian Journal for Science and Engineering, vol. 46, no. 2, pp. 1369-1382, 2021. doi:10.1007/s13369-020-05178-y

[25] S. Ayasun, Ş. Sönmez, "Gain and phase margin based stability analysis of time delayed single area load frequency control system with fractional order PI controller," Journal of the Faculty of Engineering and Architecture of Gazi University, vol. 34, no. 2, pp. 945-959, 2019. doi:10.17341/gazimmfd.460492

[26] M. A. Pakzad, S. Pakzad, M. A. Nekoui, "Exact method for the stability analysis of time delayed linear-time invariant fractional-order systems," IET Control Theory & Applications, vol. 9, no. 16, pp. 2357-2368, 2015. doi:10.1049/iet-cta.2014.1188

[27] Z. Y. Nie, Q. G. Wang, M. Wu, Y. He, "Combined gain and phase margins," ISA Transactions, vol. 48, no. 4, pp. 428-433, 2009. doi:10.1016/j.isatra.2009.07.004

[28] T. Vyhlídal, P. Zítek, "QPmR-Quasi-polynomial root-finder: Algorithm update and examples," Delay Systems, pp. 299-312, 2014. doi:10.1007/978-3-319-01695-5_22

[29] Simulink, Model-based and system-based design using Simulink, Natick, MA, USA, MathWorks, 2000

[30] S. A. Pourmousavi, M. H. Nehrir, "Introducing dynamic demand response in the LFC model," IEEE Transactions on Power Systems, vol. 29, no. 4, pp. 1562-1572, 2014. doi:10.1109/TPWRS.2013.2296696

[31] K. S. Ko, D. K. Sung, "The effect of EV aggregators with time-varying delays on the stability of a load frequency control system," IEEE Transactions on Power Systems, vol. 33, no. 1, pp. 669-680, 2017. doi:10.1109/TPWRS.2017.2690915